05,01

Changes in the ferromagnetic resonance and magnetic anisotropy spectra of multilayer heterostructures $[CoFeB/SiO_2|Bi_2Te_3]_{47}$ when applying Fe/Fe_3O_4 nanoparticles to their surface

© A.I. Bezverkhny[1,2], R.B. Morgunov[1,2,¶]

[1] Institute of Problems of Chemical Physics, Russian Academy of Sciences, Chernogolovka, Moscow oblast, Russia
[2] I.M. Sechenov First Moscow State Medical University, Moscow, Russia

¶ E-mail: morgunov2005@yandex.ru

Received April 12, 2022
Revised April 12, 2022
Accepted April 19, 2022

The ferromagnetic resonance method revealed an increase in the anisotropy constant of the heterostructure $[CoFeB/SiO_2|Bi_2Te_3]_{47}$ under the action of magnetic Fe/Fe_3O_4 nanoparticles deposited on the surface of the heterostructure by 20%. It has been established that a layer of Fe/Fe_3O_4 nanoparticles ~ 27 nm thick on a GaAs diamagnetic substrate has its own magnetic anisotropy caused by the magnetic dipole interaction between the particles. A layer of nanoparticles bound by magnetic dipole interaction forms an equivalent magnetic film, the scattering field of which changes the effective magnetic anisotropy of the heterostructure $CoFeB/SiO_2|Bi_2Te_3]_{47}$.

Keywords: ferromagnetic resonance, magnetic anisotropy, multilayer heterostructures, magnetic dipole interaction, nanoparticles.

DOI: 10.21883/PSS.2022.08.54614.344

1. Introduction

One of the modern areas in spintronics development is the creation of sensors of magnetic nanoparticles present in living cells or body tissues. High sensitivity of spin valves to local magnetic fields of nanoparticles allows for detection of a relatively small number of magnetically labelled cells (e.g. see the reviews [1,2]). Magnetic markers widely used in medicine are Fe/Fe_3O_4 nanoparticles having a considerable potential biocompatibility with various objects [3]. A local stray magnetic field generated by a separate ferromagnetic nanoparticle can switch over the direction of magnetization of thin ferromagnetic layers in a spin valve, and, thereby, it can locally change the magnetoresistance which is sensitive to magnetization of such layers. Efficiency of conversion of the local particle field into a change of sensor resistance determines the usability of multilayer platforms as sensors in biology and medicine. However, such efficiency depends not only on spin valve quality and magnetoresistance as it might seen at first sight. A significant role is played by balance between strength of the nanoparticle local field and magnetic anisotropy of sensor layers which determines the efficiency of switchover of their local magnetization. Therefore, a sensor having a very high magnetoresistance may be unusable because nanoparticles do not properly switch over the magnetization of its layers. Vice versa, a sensor efficiency gain can be obtained even when it has a low magnetoresistance but a high capability to switch over magnetization under particles' action. Therefore, the sensor industry needs spin valve platforms having the lowest possible „particle count/resistance change" coefficient.

A spin valve platform is in most cases a multilayer structure where continuous ultrathin (~ 1 nm) layers of ferromagnetic metal (frequently CoFeB) are separated by thin dielectric layers (TMR-sensors CoFeB|MgO|CoFeB [4]) or non-magnetic metal (GMR-sensors CoFeB|Ta|CoFeB [5]). In such conditions of continuous films, local magnetization reversal of CoFeB layers under a nanoparticle was found experimentally, and the obtained results were confirmed by modelling [6,7].

There are also structures where ferromagnetic layers are not continuous but consist of CoFeB islands separated by SiO_2 dielectric in the film plane. A layer of other material is present between such layers, e.g. Bi_2Te_3. Similar structures were studied in detail in a series of papers [8–15]. They have a magnetoresistance of about 6% and manifest memristive and other interesting properties. Despite a low magnetoresistance value, almost 100 times lower than the maximum obtained value in CoFeB|MgO|CoFeB structures, they can be of interest as platforms for magnetoresistive sensors. Switchover of local magnetization in continuous-film sensors involves a large portion of the ferromagnetic film material in this process, i.e. all spins of a local area of the continuous film much change their orientation [6,7]. The magnetization reversal barrier in this case is determined by magnitude of magnetic anisotropy of the film material. The following situation can occur in island films: magnetization reversal of an individual film cluster (island) is possible in a considerably smaller nanoparticle field than is necessary in a continuous film. This can be due to the

fact that the effective magnetic anisotropy of an island can be greatly reduced by surface and interface anisotropy, as well as by shape anisotropy. In this case, a loss of magnetoresistance can be compensated by a magnetization switchover efficiency gain.

We did not solve the issue of attainment of a low „particle count/resistance change“coefficient in this paper; we tried to determine the efficiency of nanoparticles' impact on switchover of magnetization of island multilayer heterostructures where thin ferromagnetic films are not continuous but consist of CoFeB alloy clusters. The paper was aimed at revealing and analysis of changes in ferromagnetic resonance spectra (FRS) in $[CoFeB/SiO_2|Bi_2Te_3]_{47}$ heterostructures upon application of ferromagnetic Fe_3O_4 nanoparticles.

2. Procedure and samples

Four samples were used in the experiments.

I. The first sample (the reference one) is a GaAs diamagnetic monocrystal, sized 2.5×4 mm and 1 mm thick. We have previously made sure that the sample and its possible admixtures do not give a magnetic resonance signal in the studied field range where the spectra were recorded.

II. The second sample consist of the above-mentioned GaAs substrate with Fe/Fe_3O_4 nanoparticles deposited on its surface. Deposition was performed using a colloidal solution of nanoparticles in toluene having the concentration of 10^{-2} g/ml. The sample surface was coated with $15\,\mu$l of the solution, so that $\sim 5 \cdot 10^{11}$ particles formed a film ~ 27 nm thick.

III. The third sample is a plate sized 3×4 mm and is a multilayer heterostructure $[(Co_{41}Fe_{39}B_{20})_x(SiO_2)_{100-x}|Bi_2Te_3]_{47}$ of 47 alternating pairs of $CoFeB/SiO_2$ and Bi_2Te_3 layers. The $CoFeB/SiO_2$ layer consists of CoFeB alloy nanoparticles distributed in the SiO_2 matrix. Weight fractions of CoFeB alloy: Co — 41%, Fe — 39%, B — 20%. Layer thickness of $CoFeB/SiO_2|CoFeB = 5.2$ nm, and layer thickness of $Bi_2Te_3/Bi_2Te_3 = 1.7$ nm. The sample preparation and evaluation procedure is detailed in [8].

IV. The fourth sample is sample III with Fe/Fe_3O_4 nanoparticles deposited on its surface. Nanoparticle concentration on the surface of the $CoFeB/SiO_2|Bi_2Te_3$ platform and deposition method were similar to the described case for sample II.

Fe/Fe_3O_4 nanoparticles dispersed in toluene were prepared commercially and evaluated at NUST MISiS. Fig. 1 shows an image of Fe/Fe_3O_4 nanoparticles on the GaAs substrate obtained in a transmission electron microscope (TEM). The average nanoparticle size is $d = 24$ nm, according to the size distribution histogram (see the inset in Fig. 1). The X-ray diffraction spectrum of Fe/Fe_3O_4 nanoparticles on the GaAs substrate (Fig. 2) contained maxima which pertain to the nanoparticle core (it consists of Fe) and maxima which pertain to the Fe_3O_4 shell. This confirms the nanoparticle structure standardized in medical-biological research.

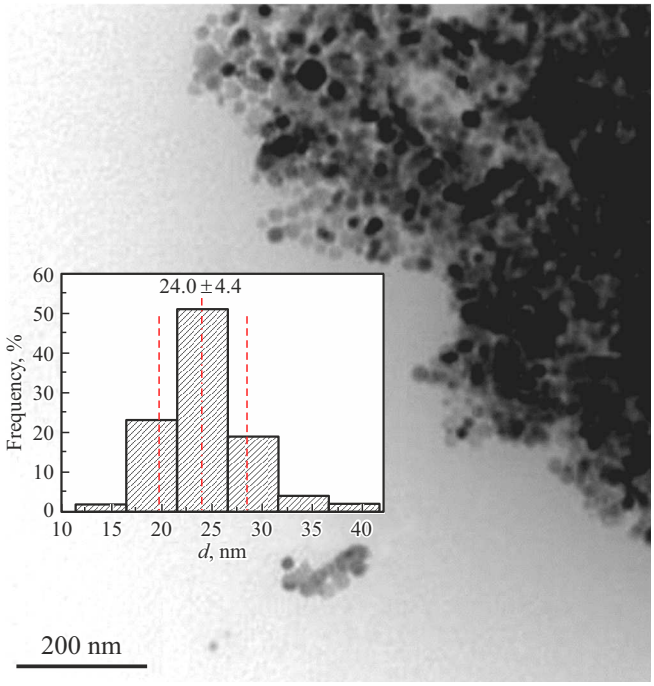

Figure 1. TEM-image of Fe/Fe_3O_4 nanoparticles. The inset shows a histogram of particle size distribution.

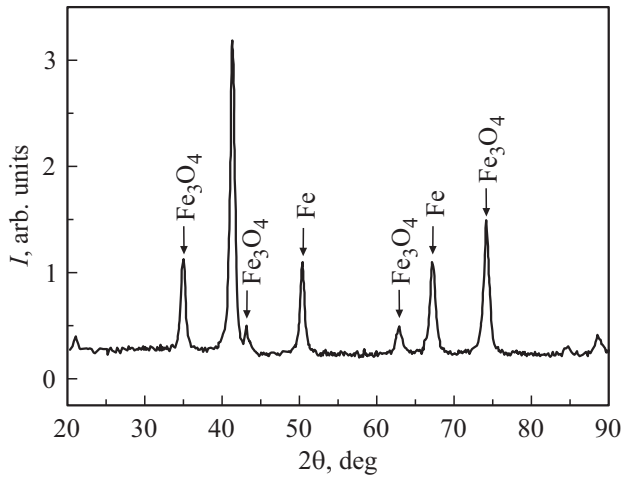

Figure 2. X-ray diffraction spectrum of Fe/Fe_3O_4 nanoparticles.

Ferromagnetic resonance was studied using an EPR10-MINI electron paramagnetic resonance spectrometer of the X-range. The microwave field frequency for all samples was 9.46 GHz, microwave radiation power was 5 mW, modulating field amplitude was 1 Oe, modulation frequency was 100 kHz, resonator Q-factor was 4000.

3. Results and discussion

Fig. 3, a shows the FMR spectra for four samples recorded in the field perpendicular to the sample, i.e. with the polar angle value $\theta = 0°$ (θ is angle between

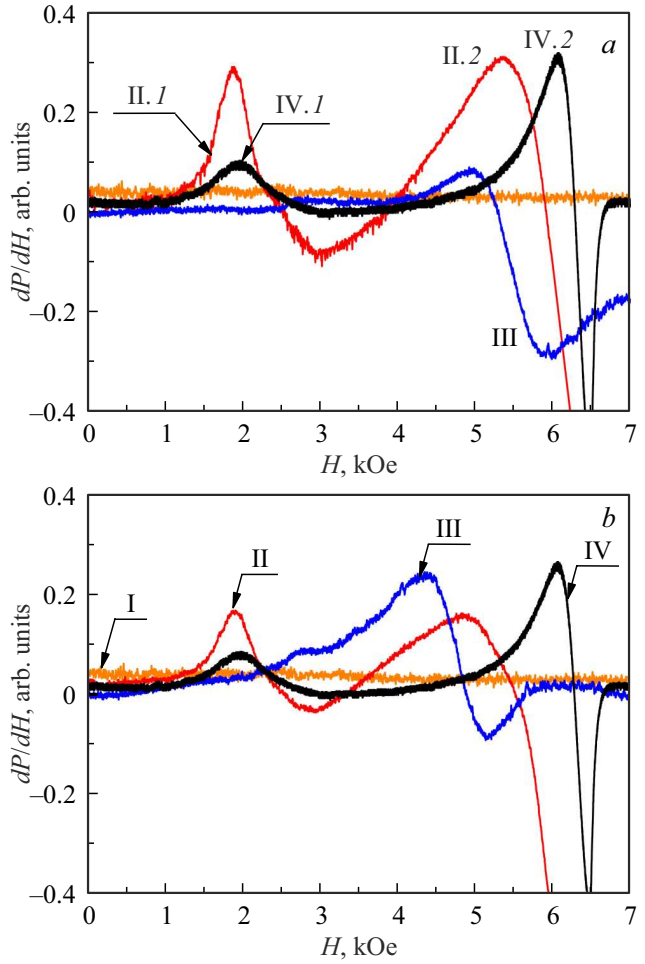

Figure 3. FMR spectra: I — GaAs, II — Fe_3O_4 nanoparticles on the GaAs substrate, III — sample CoFeB/SiO_2|Bi_2Te_3, IV — sample CoFeB/SiO_2|Bi_2Te_3 with Fe_3O_4 nanoparticles deposited on the surface, (*a*) for the polar angle $\theta = 0°$; (*b*) for the polar angle $\theta = 10°$. In Fig. 4, *a* — *1* and *2* are two resonance lines of spectrum I; *A* and *B* are two resonance lines of spectrum IV. Lines *1*, *2*, *A* and *B* are discussed in the text.

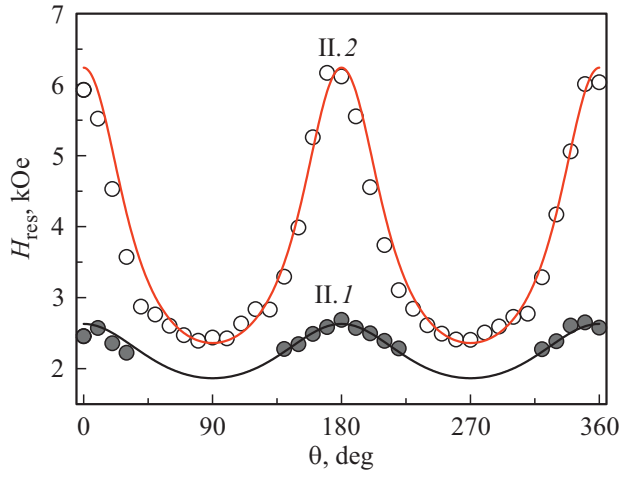

Figure 4. Resonance field H_{res} for lines II.*1* and II.*2* vs. polar angle θ for the layer of Fe_3O_4 nanoparticles on the GaAs substrate (sample II). The continuous lines show the simulations by means of equation (1).

the normal to the sample surface and the spectrometer field). A signal was not found for sample I (pure GaAs) in the whole range of angles θ. The FMR spectrum of sample II (GaAs with nanoparticles) contained two lines II.*1* and II.*2*. The spectrum of sample III (a heterostructure without particles) had one line. The spectrum of sample IV (a heterostructure with nanoparticles) contained lines IV.*1* and IV.*2*. The pair of lines in the spectrum of Fe/Fe_3O_4 nanoparticles is known well from literature and fits the spin-wave modes arising during interaction of the nanoparticle core and shell [16].

A small change in the polar angle to $\theta = 10°$ causes a significant shift of all spectrum lines, except the background spectrum of sample I (Fig. 3, *b*). Not only the spectra of a heterostructure and a heterostructure with particles, but also the spectrum of Fe/Fe_3O_4 nanoparticles on the GaAs substrate turn out to be anisotropic. It means that particle density on the substrate is high enough to form a layer with magnetic anisotropy on a diamagnetic substrate.

The angular dependences of resonance field $H_{res}(\theta)$ for lines II.*1* and II.*2* are shown in Fig. 4. Though the resonance field was determined by decomposing the spectrum into Lorentz lines, execution of this algorithm was hindered in the line overlap region where the spectrum approximation was ambiguous. Therefore, some points are absent on the angular dependence of line II.*1*. The angular dependences were analyzed using a formula which describes the magnetic anisotropy of a film with cubic symmetry [17]:

$$(\omega_0/\gamma)^2 = (H_{res} \cdot \cos(\theta_M - \theta) - 4\pi M_{eff} \cdot \cos^2\theta)$$

$$\times (H_{res} \cdot \cos(\theta_M - \theta) - 4\pi M_{eff} \cdot \cos(2\theta_M) + H_{2\|}), \quad (1)$$

where $\omega_0 = 9.46$ GHz is spectrometer resonance frequency, γ — gyromagnetic ratio, H_{res} — resonance field of FMR line, $4\pi M_{eff} = -2(K_b + K_S)/M_S + 4\pi M_S$ — effective field, $K_b + K_S = K_{eff}$ (where K_b is the volume anisotropy constant, K_S — surface anisotropy constant), θ — angle between the normal to the sample surface and direction of spectrometer magnetic field, θ_M — angle between the normal to the sample surface and magnetization vector, $H_{2\|}$ — first-order anisotropy field in the film plane. Magnetic anisotropy of the nanoparticle layer on the diamagnetic substrate means that the system must be described using a ratio for films and not for individual particles, though such an approximation is conventional.

The saturation magnetization in equation (1) might be the value $M_S = 340\,\text{emu/cm}^3$ which we have found for Fe/Fe_3O_4 nanoparticles on the GaAs substrate by SQUID-magnetometry in independent experiments. This value was an intermediate one between the known saturation magnetization $M_S = 220\,\text{emu/cm}^3$ for Fe_3O_4 nanoparticles [18], and saturation magnetization $M_S = 440\,\text{emu/cm}^3$ known for similarly sized ferrum nanoparticles [19]. Though the found value $M_S = 340\,\text{emu/cm}^3$ agrees well with the presence of a Fe core and a Fe_2O_4 shell in Fe/Fe_2O_4 nanoparticles, the question arises as to which of the two lines should be simulated by equation (1) with the above-mentioned value of saturation magnetization. The studies of

Fe/Fe_2O_4 nanoparticles have shown that their FMR-spectra contain two lines present due to the spin-wave modes which result from the interaction of the core and the shell [16]. Therefore, we assumed that lines II.*1* and II.*2* in Fig. 4 correspond to the signals of the ferrum core and oxide shell respectively. It should be noted that the difference of our experiments from [16] is in the fact that nanoparticle density and count in our experiments were high enough and their magnetic dipole interaction caused anisotropy of the nanoparticle layer even on a diamagnetic substrate.

The angular dependence of line II.*1* was simulated using $M_S = 440$ emu/cm^3 for Fe, and the obtained anisotropy constant was $K_{eff} = 1.04 \cdot 10^5$ erg/cm^3 and $g = 3.6$. The angular dependence of line II.*2* was simulated using $M_{S2} = 220$ emu/cm^3 for Fe_2O_4, and the obtained anisotropy constant was $K_{eff} = 3.9 \cdot 10^5$ erg/cm^3 and $g = 1.94$. The obtained values are close to the published value of magnetic anisotropy for Fe_2O_4 nanoparticles, which are within $K_{eff} = 3.2-3.5 \cdot 10^5$ erg/cm^3 [20]. Probably, these lines in the core–shell system cannot be mechanically attributed to the core and shell as non-interacting isolated subsystems. We think it is more correct to speak of spin-wave modes arising in a complex compound particle.

Sample III has one resonance line on the FMR spectrum (see Fig. 3). The angular dependence of the resonance field of this line $H_{res}(\theta)$ and its simulation by means of equation (1) are shown in Fig. 5. Saturation magnetization $M_S = 500$ emu/cm^3 for sample $CoFeB/SiO_2|Bi_2Te_3$ (sample III) has been obtained earlier in [21]. A simulation of dependence $H_{res}(\theta)$ for sample III has provided the following parameters $K_{eff} = 6.2 \cdot 10^5$ erg/cm^3, $g = 1.98$, which are typical for CoFeB films.

The main object of interest is sample IV, being a multilayer platform with a layer of nanoparticles. In such a system we might anticipate a summation of signals from the nanoparticle layer (lines II.*1* and II.*2*) and the platform signal (line III). However, sample IV has only two resonance lines IV.*1* and IV.*2* (see Fig. 3, *a*). The resonance field of line IV.*1* does not greatly depend on angle θ, while the resonance field of line IV.*2* greatly depends on the angle (Fig. 6). On the whole, the spectrum and its angular dependence of FMR of the lines of the given sample resemble the spectrum and the angular dependence of resonance fields of the FMR lines of sample II. A comparison of the angular dependences of lines II.*1* and IV.*1* (see Fig. 6) suggests that the resonance fields of these lines are close in the whole range of the studied angles. It might be assumed that there is additive summation of lines II.*2* from the nanoparticle layer and line III of the platform itself. However, a considerable change in the orientation dependence of line IV.*1* (Fig. 6) as compared to dependence II.*1* (Fig. 4) prevents from accepting this viewpoint. Thus, a sample with a ferromagnetic platform and nanoparticles features a non-additive summation of signals, which means interaction of the nanoparticle layer and the platform.

The greatest changes that mean a non-additive summation of the spectra of the nanoparticle layer and the ferromagnetic platform have been revealed when comparing the angular dependences of spectrum line widths $H_{p-p}(\theta)$ (Fig. 7). It can be seen that, though the orientation dependences of width of line II.*1* which pertains to nanoparticles (dependence 1 in Fig. 7) and line III which pertains to the ferromagnetic platform (dependence 2 in Fig. 7), are similar, a combined system of particles and platform (dependence 3 in Fig. 7) features the dependence $H_{p-p}(\theta)$ which cannot be explained by summation of orientation dependences of the line widths of the initial system components.

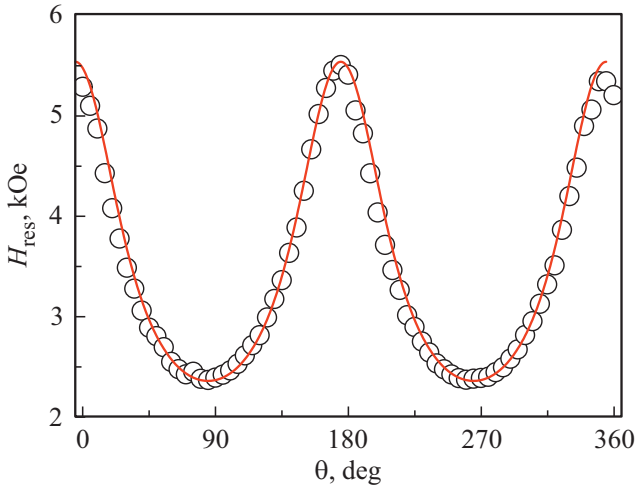

Figure 5. Resonance field H_{res} vs. polar angle θ for sample III. The continuous line shows the simulation by means of equation (*1*).

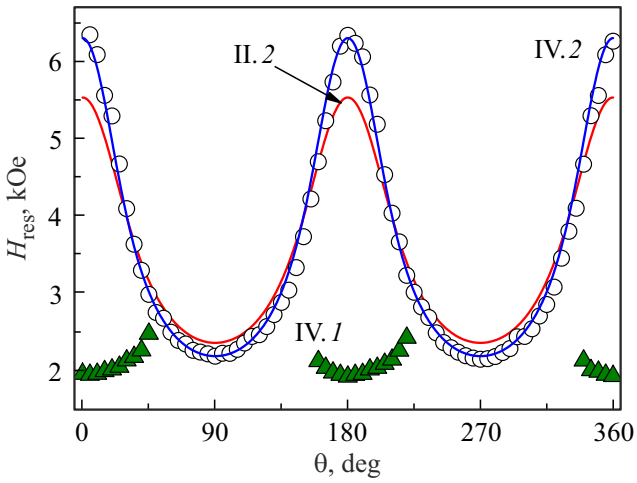

Figure 6. Resonance fields H_{res} vs. polar angle θ for lines IV.*1* and IV.*2*, for sample IV ($CoFeB/SiO_2|Bi_2Te_3$ coated with Fe_3O_4 nanoparticles). The continuous blue line shows the simulation of angular dependence of line IV.*2* by means of equation (1) and the simulation of line II.*2* for nanoparticles on a diamagnetic substrate (Fig. 4) is shown for comparison.

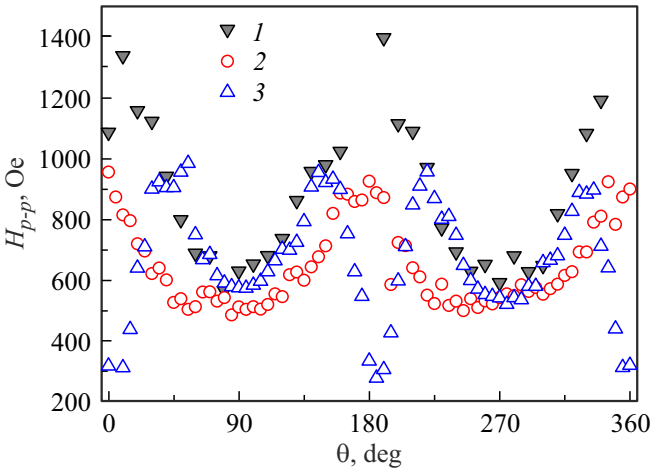

Figure 7. Widths of FMR lines vs. polar angle θ: *1* — for nanoparticles on the GaAs surface (sample II), *2* — for a pure ferromagnetic platform (sample III), *3* — for resonance line VI.*2* of the ferromagnetic platform coated with nanoparticles.

Paper [7] described the impact of nanoparticles on FMR spectra in single-crystal continuous CoFeB|Ta|CoFeB platforms. The effect consisted only in a 20% change of the amplitude of angular dependence of the resonance field for the platform FMR line. This is a rather small effect that cannot be easily used in practice to create particle sensors on a platform. The results presented in this paper show that a considerably higher sensitivity can be attained by selecting an operating field in the resonance region in such a way that a line width change can change the microwave absorption of the „platform−particle“system many times. The obtained results apply to the case of high nanoparticle concentrations and, probably, cannot be used when rare magnetically labelled biological objects are located on the sensor surface. However, a comparison with continuous platforms shows that we have attained a higher sensitivity and more drastic changes of angular dependences of FMR lines than with the use of continuous platforms. This is explained by the fact that reverse magnetization of ferromagnetic islands of CoFeB films by the nanoparticle scattering field is easier. The effect might be also increased in a certain extent due to the use of multilayer platforms in our experiments.

4. Conclusions

1. Fe/Fe_2O_4 nanoparticles have two resonance lines with $g = 3.6$ and $g = 1.94$, caused by the excitation of spin-wave modes in a complex shell−core system. Magnetic dipole interaction between nanoparticles occurs in the layer and causes magnetic anisotropy of the layer even if it is deposited on a diamagnetic substrate.

2. Deposition of a layer of Fe/Fe_2O_4 nanoparticles on a ferromagnetic $CoFeB/SiO_2|Bi_2Te_3$ substrate results in a change of the particles' orientation dependence of the resonance field of FMR lines, which indicates an impact of the ferromagnetic platform on the particles' FMR spectrum.

3. A sample consisting of a ferromagnetic substrate with a deposited nanoparticle layer also features a change in the angular dependence of the line width which cannot be explained by overlapping of the lines of the substrate and the nanoparticle layer. This suggests an impact of nanoparticles on FMR in the substrate. The resultant anisotropy constant for a platform with nanoparticles is $\sim 20\%$ greater that the anisotropy constant for a pure $CoFeB/SiO_2|Bi_2Te_3$ substrate.

Funding

The work has been performed within the thematic chart of the Institute of Problems of Chemical Physics AAAA-A19-119092390079-8.

Conflict of interest

The authors declare that they have no conflict of interest.

References

[1] I. Koh, L. Josephson. Sensors **9**, *10*, 8130 (2009).
[2] V. Fernandes Cardoso, A. Francesko, C. Ribeiro, M. Bañ obre-López, P. Martins, S. Lanceros-Mendez. Adv. Healthcare Mater. **7**, *5*, 1700845 (2017).
[3] A. Van de Walle, J.E. Perez, A. Abou-Hassan, M. Hemadi, N. Luciani, C. Wilhelm. Mater. Today Nano **11**, 100084 (2020).
[4] S. Ikeda, J. Hayakawa, Y. Ashizawa, Y.M. Lee, K. Miura, H. Hasegawa, M. Tsunoda, F. Matsukura, H. Ohno. Appl. Phys. Lett. **93**, *8*, 082508 (2008).
[5] R.B. Morgunov, G.L. L'vova, A.D. Talantsev, Y. Lu, X. Devaux, S. Migot, O.V. Koplak, O.S. Dmitriev, S. Mangin. Thin Solid Films **640**, 8 (2017).
[6] R.B. Morgunov, O.V. Koplak, R.S. Allayarov, E.I. Kunitsyna, S. Mangin. Appl. Surf. Sci. **527**, 146836 (2020).
[7] E.I. Kunitsyna, R.S. Allayarov, O.V. Koplak, R.B. Morgunov, S. Mangin. ACS Sens. **6**, *12*, 4315 (2021).
[8] O.V. Dunets, Yu.E. Kalinin, M.A. Kashirin, A.V. Sitnikov. ZhTF **83**, *9*, 114 (2013) (in Russian).
[9] E.N. Kablov, O.G. Ospennikova, V.P. Piskorsky, D.V. Korolev, Yu.E. Kalinin, A.V. Sitnikov, E.I. Kunitsyna, A.D. Talantsev, V.L. Berdinsky, R.B. Morgunov. FTT **58**, *6*, 1086 (2016) (in Russian).
[10] E.P. Domashevskaya, N.A. Builov, V.A. Terekhov, K.A. Barkov, V.G. Sitnikov. FTT **59**, *1*, 161 (2017) (in Russian).
[11] O.V. Gerashchenko, V.A. Ukleyev, E.A. Dyadkina, A.V. Sitnikov, Yu.E. Kalinin. FTT 59, **1**, 157 (2017) (in Russian).
[12] V.V. Rylkov, S.N. Nikolaev, V.A. Demin, A.V. Emelyanov, A.V. Sitnikov, K.E. Nikiruy, V.A. Levanov, M.Yu. Presnyakov, A.N. Taldenkov, A.L. Vasiliev, K.Yu. Chernoglazov, A.S. Vedeneev, Yu.E. Kalinin, A.B. Granovsky, V.V. Tugushev, A.S. Bugaev. J. Exp. Theor. Phys. **126**, *3*, 353 (2018).
[13] K.E. Nikiruy, A.V. Yemelyanov, V.A. Demin, V.V. Rylkov, A.V. Sitnikov, P.K. Kashkarov. Pis'ma v ZhTF **44**, *10*, 20 (2018) (in Russian).
[14] H. Al Azzawi, Yu. Kalinin, A. Sitnikov, O. Tarasova. Solid State Phenomena **233−234**, 467 (2015).
[15] V. Ukleev, E. Dyadkina, A. Vorobiev, O.V. Gerashchenko, L. Carond, A.V. Sitnikov. J. Non-Cryst. Solids **432**, 499 (2016).

[16] P.V. Finotelli, M.A. Morales, M.H. Rocha-Leão, E.M. Baggio-Saitovitch, A.M. Rossi. Mater. Sci. Eng. C **24**, *5*, 625 (2004).
[17] C. Kittel. Phys. Rev. **73**, *2*, 155 (1948).
[18] G.S. Shahane, K.V. Zipare, R.P. Pant. Magnetohydrodynamics **49**, *3–4*, 317 (2013).
[19] A. Matsumoto, T. Sugiura, M. Kobashi, S. Yamamoto. Mater. Transact. **61**, *7*, 1404 (2020).
[20] E. Lima Jr, A.L. Brandl, A.D. Arelaro, G.F. Goya. J. Appl. Phys. **99**, *8*, 083908 (2006)
[21] A.I. Bezverkhniy, A.D. Talantsev, Yu.E. Kalinin, A.V. Sitnikov, V.A. Nikitenko, O.V. Koplak, O.S. Dmitriyev, R.B. Morgunov. FTT **61**, *2*, 266 (2019) (in Russian).